

1 **Title:** Beta-cell Cre expression and reduced *Ins1* gene dosage protect mice from type 1 diabetes

2

3 **Authors:** Søs Skovsø^{1*}, Peter Overby^{1*}, Jasmine Memar-Zadeh¹, Jason T.C. Lee¹, Jenny C.C. Yang¹,
4 Iryna Shanina¹, Vaibhav Sidarala², Elena Levi-D'Ancona², Jie Zhu², Scott A. Soleimanpour², Marc S.
5 Horwitz¹, James D. Johnson^{*1}

6

7 * These authors contributed equally

8 Correspondence should be addressed to James D. Johnson: james.d.johnson@ubc.ca, 2350 Health
9 Sciences Mall, 5358 Life Sciences Building, Vancouver, BC, V6T 1Z3

10

11 **Affiliations:** ¹ Life Sciences Institute, University of British Columbia, Vancouver, BC, Canada; ²
12 Department of Molecular and Integrative Physiology, Division of Metabolism, Endocrinology, and
13 Diabetes of the Department of Internal Medicine, University of Michigan, Ann Arbor, MI, USA

14

15 **Correspondence:** J.D.J.

16

17 **Keywords:** type 1 diabetes animal models, Cre recombinase, knock-in mice, pancreatic β -cell

18

19 **Funding:** This project was primarily supported by an operating grant to J.D.J. from the Canadian
20 Institutes for Health Research (PJT-152999) and the JDRF Centre of Excellence at UBC (3-COE-2022-
21 1103-M-B). S.A.S. was supported by the JDRF (CDA-2016-189, COE-2019-861), the NIH (R01
22 DK108921, U01 DK127747), and the Department of Veterans Affairs (I01 BX004444).

23

24 **Acknowledgements:** We thank colleagues in the β -cell biology field for helpful discussions, including
25 on Twitter.

26

27 **Disclosure statement:** The authors have nothing to disclose

28

29 **Author Contributions**

30 S. S. co-conceived experiments, designed and executed *in vivo* experiments, analyzed data, co-wrote
31 the manuscript

32 P. O. executed *in vivo* experiments, analyzed data, co-wrote the manuscript

33 J. M-Z. analyzed data and co-wrote the manuscript

34 J. L. designed and analyzed flow cytometry experiments

35 J. C.C Y. executed *in vivo* experiments

36 I. S. designed and executed flow cytometry experiments

37 V. S. conducted *in vivo* validation experiments

38 E. L-D. conducted *in vivo* validation experiments

39 J. Z. conducted *in vivo* validation experiments

40 S. A. S. oversaw and interpreted *in vivo* validation experiments

41 M. H. oversaw and interpreted *in vivo* experiments

42 J. D. J. designed the model, co-conceived experiments, analyzed data, co-wrote the manuscript, and is
43 the ultimate guarantor of this work.

44

45

46 **Abstract word count:** 222

47 **Body word count:** 4023

48 **Reference count:** 38

49 **Figure count:** 6

50

51

52

53

54

55

56 **Abstract**

57 A central goal of physiological research is the understanding of cell-specific roles of disease-
58 associated genes. Cre-mediated recombineering is the tool of choice for cell type-specific analysis of
59 gene function in pre-clinical models. In the type 1 diabetes research field, multiple lines of NOD mice
60 have been engineered to express Cre recombinase in pancreatic β -cells using insulin promoter
61 fragments, but tissue promiscuity remains a concern. Constitutive *Ins1*^{tm1.1(cre)Thor} (*Ins1*^{Cre}) mice on the
62 C57/bl6-J background has high β -cell specificity and with no reported off-target effects. We explored if
63 NOD:*Ins1*^{Cre} mice could be used to investigate β -cell gene deletion in type 1 diabetes disease modeling.
64 We studied wildtype (*Ins1*^{WT/WT}), *Ins1* heterozygous (*Ins1*^{Cre/WT} or *Ins1*^{Neo/WT}), and *Ins1* null (*Ins1*^{Cre/Neo})
65 littermates on a NOD background. Female *Ins1*^{Neo/WT} mice exhibited significant protection from diabetes,
66 with further near-complete protection in *Ins1*^{Cre/WT} mice. The effects of combined neomycin and Cre
67 knock-in in *Ins1*^{Neo/Cre} mice were not additive to the Cre knock-in alone. In *Ins1*^{Neo/Cre} mice, protection
68 from diabetes was associated with reduced insulitis at 12 weeks of age. Collectively, these data confirm
69 previous reports that loss of *Ins1* alleles protects NOD mice from diabetes development and
70 demonstrates, for the first time, that Cre itself may have additional protective effects. This has significant
71 implications for the experimental design and interpretation of pre-clinical type 1 diabetes studies using
72 β -cell-specific Cre in NOD mice.

73

74

75 **Introduction**

76 Type 1 diabetes (T1D) is a chronic disorder precipitated by immune-mediated pancreatic β -cell
77 destruction and associated with the presence of autoantibodies against β -cell proteins (1,2). Due to the
78 progressive loss of β -cells and consequent insulin deficiency, individuals living with type 1 diabetes have
79 lifelong dependency on exogenous insulin (3). Higher levels of endogenous insulin secretion are
80 associated with better short- and long-term outcomes in type 1 diabetes. Preservation of residual β -cells
81 and islet function at the time of diagnosis is therefore imperative (4).

82 Exogenous insulin administration is not a cure of type 1 diabetes. Research efforts using pre-clinical
83 animal models continue to produce new therapeutic possibilities. Initially developed as a model for
84 spontaneous onset of cataracts, the female non-obese diabetic (NOD/ShiLt) mouse (commonly known
85 as NOD) is the most well-established and extensively used model of type 1 diabetes (5). The polygenic
86 NOD mouse model recapitulates multiple pathophysiological features of human type 1 diabetes,
87 including the development of autoantibodies in prediabetic NOD mice (6), circulating autoreactive T cells
88 (7), and subsequent onset of hyperglycemia as progressive β -cell loss materializes (8). While the
89 emergence of hyperglycemia most often occurs between 12-15 weeks of age, islet immune infiltration
90 is established earlier at 8-12 weeks with insulitis present across the pancreas(9). The cleanliness of
91 housing facilities and the animal breeding approach are just two factors which affect the age at which
92 these features present.

93 Mice express two nonallelic insulin genes. The insulin 2 gene (*Ins2*) is the murine homologue of the
94 human insulin gene and is located on chromosome 7 (10). The insulin 1 gene (*Ins1*) is the result of an
95 RNA-mediated gene duplication event. *Ins1* has a simpler gene structure lacking the second intron
96 present in *Ins2*, and is found on the murine chromosome 19 (10). *Ins1* is expressed specifically in
97 pancreatic β -cells, whereas *Ins2* is expressed predominantly in β -cells, with trace expression in other
98 tissues including thymus and brain (11). Previous studies have examined the effects of insulin gene
99 knockout in NOD mice. Complete knockout of *Ins2* on the NOD background accelerated diabetes onset
100 (2), a phenomenon attributed to a failure in central tolerization to insulin. Thymus-specific deletion of
101 *Ins2* was reported to be sufficient to cause spontaneous diabetes, even outside the NOD background
102 (12). Although we have not observed autoimmune diabetes in globally deficient *Ins2*^{-/-} mice (13,14) it
103 has previously reported that male, but not female, NOD:*Ins1*^{Neo/WT};*Ins2*^{-/-} mice, with a single remaining
104 *Ins1* allele have been shown to succumb to insulin insufficiency (15), a finding we confirmed on other
105 backgrounds (16). These observations were found to be dependent on housing conditions (11). In
106 contrast, NOD:*Ins1*^{Neo/Neo} mice have previously been shown to be largely protected from insulitis
107 diabetes (10), which was proposed to be due to the loss of autoantigenic *Ins1*-derived peptides despite
108 presence of insulin autoantibodies (IAA). Insulin is a primary auto-antigen in both murine and human

109 type 1 diabetes pathogenesis (1). Replacing *Ins1* with non-antigenic human insulin also protects NOD
110 mice from onset of diabetes (17). Together, these previous observations indicate that insulin 1 gene
111 dosage is a key driver of diabetes in NOD mice.

112 To advance the understanding of the underlying mechanisms of T1D pathogenesis, powerful genetic
113 engineering tools are employed by researchers across the world. *Ins1*^{Cre} mice take advantage of the
114 tissue specificity of *Ins1* expression to excise *loxP* site-flanked (floxed) DNA segments. As the Cre DNA
115 recombinase allele is inserted into exon 2 of *Ins1* in these mice, floxed target genes are removed
116 specifically in beta-cells at the cost of the loss of 1 *Ins1* allele. Both *Ins1*^{Cre} and *Ins1*^{Neo} mice have
117 reduced *Ins1* gene dosages with 50% or 100% in their heterozygous and homozygous states,
118 respectively. For *Ins1*^{Neo} mice, the neomycin cassette obliterates the entire *Ins1* promotor and gene
119 sequence in addition to deletion of 7-9kb upstream and downstream of *Ins1* (see Figure 1A).

120 Since the early days of Cre/loxP system usage, concerns of side effects such as Cre toxicity have
121 been raised. More than two decades ago, Loonstra *et al* observed increased sister chromatid exchange
122 frequency, leading to a cellular halt in the G₂/M phase and a reduction in proliferation of mouse
123 embryonic fibroblasts (MEF) transduced with a bicitronic retroviral vector encoding Cre (18). Silver and
124 Livingston demonstrated similar results including ceased proliferation in 293xLac cells, NIH 3T3 cells
125 and MEFs transfected with Cre-expressing retroviral vectors (19). The same study revealed
126 chromosomal abnormalities in Cre-expressing MEFs. Lentiviral Cre administration and expression have
127 likewise been shown to reduce proliferation through cellular accumulation in the G₂M phase of Cre-
128 expressing CV-1 and COS cells, two kidney cell lines derived from monkeys (20). Cre toxicity has been
129 shown to be dose dependent, even when expressed transiently, when using an adenovirus vector (21).
130 Past studies have confirmed Cre toxicity and apoptosis in mouse cardiac tissue (22,23) and p53^{-/-} thymic
131 lymphoma cells (24). Collectively, these findings emphasize the necessity of using Cre-only (no flox)
132 controls into *in vivo* research study designs since Cre recombinase expression may affect cells beyond
133 the intended target gene deletion.

134 For this study, we generated and characterized a new NOD *Ins1*^{Cre} knock-in mouse line. Our
135 intension was to establish an *in vivo* tool facilitating the unravelling of type 1 diabetes pathogenesis. The

136 NOD *Ins1*^{Cre} model would ideally enable studying of β-cell specific deletion of target genes in mice on
137 an NOD background. As a predecessor, the goal of this study was to investigate the impact of 1) deleting
138 one *Ins1* allele and 2) introducing beta cell specific Cre expression, on the spontaneous diabetes
139 development NOD mice are well known for. As previous studies by the Eisenbarth group provided
140 evidence that *Ins1*^{Neo/WT} mice, with only one intact *Ins1* allele, exhibit decreased and delayed diabetes
141 incidence, we were expecting similar results for *Ins1*^{Cre/WT} mice. We incorporated both NOD:*Ins1*^{Neo/WT}
142 NOD;*Ins1*^{WT/WT} littermates in our study design, to control for both the loss of one *Ins1* allele and
143 introduction of Cre expression in NOD *Ins1*^{Cre/WT} mice. We compared diabetes incidence, insulitis
144 severity, and immune activation between groups within each sex. Our data demonstrate that *Ins1*-driven
145 Cre expression has further protective effects beyond the loss of a single *Ins1* allele deleted via *Ins1*^{Neo}.
146 Carefully chosen proper controls and caution are therefore required when interpreting experiments
147 including β-cell specific Cre expression in mice on an NOD background.

148

149 **Methods**

150 *Mice*

151 All animal procedures and ethical standards were in accordance with the Canadian Council for
152 Animal Care guidelines. All animal studies and protocols were approved by the University of British
153 Columbia Animal Care Committee and Institutional Care and Use Committee (IACUC) at the University
154 of Michigan. At UBC, mice were housed in the Centre for Disease Modelling Specific Pathogen-Free
155 (SFP) facility on a standard 12-h light/12-h dark cycle with ad libitum access to chow diet (PicoLab,
156 Mouse Diet 20–5058). To generate NOD:*Ins1*^{Cre} and NOD:*Ins1*^{Neo} mice, we contracted The Jackson
157 Laboratories to backcross (>12 times) B6(Cg)-*Ins1*^{tm1.1(cre)Thor}/J (The Jackson Laboratory, US,
158 #026801) (*Ins1*^{Cre}) and NOD.129S2(B6)-*Ins1*^{tm1Jja}/GseJ (The Jackson Laboratory, US, #0005035)
159 *Ins1*^{Neo}) mice onto a NOD/ShiLtJ (The Jackson Laboratory, US, #001976) (NOD) background. The
160 *Ins1*^{Cre} and *Ins1*^{Neo} mice were originally on a mixed, largely C57Bl/6J, background. Subsequently, we
161 designed a strict breeding strategy for our study. An *Ins1*^{Cre} maternal parent colony as well as a *Ins1*^{Neo}
162 paternal parent colony was established (Fig. 1B). Each parent colony was backcrossed every five

163 generations. Female *Ins1*^{Cre/WT} and male *Ins1*^{Neo/WT} mice were set up as breeders, at 7-8 weeks of age,
164 to generate experimental mice. Mice from the parental colonies were only included once as breeders to
165 eliminate risk of onset of hyperglycemia during pregnancy and weaning at later ages. This breeding
166 strategy generated littermates of four genotypes: wildtype NOD:*Ins1*^{WT/WT} mice with both insulin 1
167 alleles, heterozygous NOD:*Ins1*^{Cre/WT} mice with an *Ins1* replaced with Cre-recombinase, heterozygous
168 NOD:*Ins1*^{Neo/WT} mice with one *Ins1* allele replaced with a neomycin cassette, and full *Ins1* null mice with
169 both *Ins1* alleles replaced NOD:*Ins1*^{Neo/Cre}. Specific cohorts were monitored twice per week for the sole
170 purpose of determining hyperglycemia onset incidence and body mass changes. Any mice that
171 developed diabetes, defined as two consecutive blood glucose measurements ≥ 16 mmol/L or one
172 measurement ≥ 22 mmol/L, were euthanized. Specific cohorts were generated for tissue analysis
173 terminated at 12 weeks of age in a pre-diabetic phase (for the Vancouver housing facility) or at 1 year
174 of age, all animals were monitored for diabetes prior to euthanasia.

175 An additional colony of NOD:*Ins1*^{Cre} mice were generated independently through in-house
176 backcrossing at a second site (University of Michigan) via the speed congenic approach in consultation
177 with Charles River Laboratories (Wilmington, MA). Following each backcross, *Ins1*^{Cre/WT} offspring with
178 allelic profiles most closely matching the NOD strain (determined by MAX-BAX mouse 384 SNP panel
179 screening), were selected as breeders for the subsequent backcross. Following 8 generations of
180 backcrossing, animals with an allelic profile percent match $>99.9\%$ were utilized to generate *Ins1*^{WT/WT}
181 and *Ins1*^{Cre/WT} experimental mice. Animals were housed in an SPF facility on a standard 12-h light/12-h
182 dark cycle with access to ad libitum chow diet (LabDiets, Rodent Diet 5L0D) and water. Drinking water
183 was provided at a pH level of 2.5-3 upon advice from Jackson laboratories that acidified water supports
184 the diabetes frequency in many NOD colonies (25). Blood glucose measurements were taken once-twice
185 per week. Incidence of diabetes, defined as blood glucose levels > 16 mM for 5 consecutive
186 measurements, was recorded. Diabetic mice were euthanized and excluded from future analysis.

187 *Tissue processing and histology*

188 Immediately following euthanasia, pancreata were collected according to a pre-established protocol
189 with the exception that extracted pancreases were not further treated to obtain isolated islets and were

190 instead processed as a whole(26). The dissected pancreata were fixed in 4% PFA for 24 hours prior to
191 storage in 70% ethanol at 4 °C. Paraffin-embedded sections were prepared, stained with hematoxylin
192 and eosin (H&E), and imaged by WaxIT Histology Services Inc. (Vancouver, BC).

193

194 *Islet infiltration scoring*

195 Images from H&E-stained pancreatic sections were analyzed with QuPath software (27). Islets in
196 pancreatic sections were scored blindly for pancreatic islet infiltration of mononuclear immune cells
197 according to the previously established 4-point scale(28). In brief, 0- no insulitis, 1- peri-insulitis marked
198 by less than 25% peripheral immune-islet infiltration, 2- insulitis marked by 25-75% immune cell
199 infiltration, 3- severe insulitis marked by greater than 75% immune-islet infiltration. Random samples
200 were scored by a second person to ensure consistency. 25-30 islets per mouse.

201

202 *Insulin auto-antibodies and plasma insulin*

203 Blood for plasma insulin and autoantibodies measurements was collected at study endpoint by cardiac
204 puncture from anesthetized Animals (2.5% isoflurane) and put directly on ice. Insulin plasma where
205 measured using Mouse Insulin ELISA kit (#80-INSMS-E10, RRID: AB_2923075; ALPCO). Samples
206 were shipped to the Insulin Antibody Core Lab at the University of Colorado, Barbara Davis Diabetes
207 Centre for auto-antibody analysis. The IAA data are expressed as an index against a standard
208 positive and negative controls as procedure at the Insulin Antibody Core lab

209

210 *Flow cytometry*

211 Immediately following euthanasia lymph nodes and spleen were isolated and splenic single-cell
212 suspensions were counted and stained with fluorescently conjugated monoclonal antibodies (mAbs)
213 for cell-surface markers (see Table 1 for list of antibodies used). Fixable Viability Dye eFluor™ 506
214 was used as viability dye (#65-0866-14; ThermoFischer). Following staining, cells were analyzed by
215 flow cytometry and Flow Jo software (Tree Star Inc., Ashland, Oregon).

216

217 **Statistics**

218 Statistical significance was assessed using 2-way ANOVA analysis with Tukey's multiple
219 comparisons test, at a threshold of $p < 0.05$. Plasma insulin, Insulitis and insulin auto-antibodies
220 significance were quantified by 1-way ANNOVA analyses. We used the Mantel-Cox-log rank test,
221 corrected with the Benjamini-Hochberg procedure, to analyse the Kaplan Meier survival plots. Repeated
222 measured Mixed effect models were applied for RBG and Body mass analyses.

223 Prism 9 (GraphPad Software Inc., USA) was used for statistical analyses and generation of most
224 figure panels. Data are expressed as mean \pm SEM unless otherwise specified.

225

226

227 **Results**

228 *Type 1 diabetes incidence*

229 A greater proportion of female, in comparison to male, mice develop diabetes and the timing of the
230 development of the disease is more consistent. We observed the highest diabetes incidence in female
231 NOD:*Ins1*^{WT/WT} mice, with 65% diabetes incidence at 1 year (Fig. 1C). The majority of these mice (7/9)
232 were diabetic before 20 weeks of age. The diabetes incidence and disease time-course of this study
233 was comparable with previous NOD:*Ins1*^{WT/WT} cohorts in our facilities (28), although slightly delayed
234 relative to some other facilities (see below). Female NOD:*Ins1*^{Cre/WT} exhibited both a delay in diabetes
235 onset and a diabetes incidence by the end of the study of only 27%, which was significantly different
236 when compared to NOD:*Ins1*^{WT/WT} mice at one year of age ($p=0.033$; $p_{\text{adjust}}=0.078$; Fig. 1C). We also
237 observed a delay in the timing of the onset between female NOD:*Ins1*^{Neo/WT} mice (Fig. 1C), in agreement
238 with previous studies of NOD:*Ins1*^{Neo/WT} mice (10), but there was no difference in the final diabetes
239 incidence between female littermate NOD:*Ins1*^{Neo/WT} mice (64%) and NOD:*Ins1*^{WT/WT} mice (64%)
240 ($p=0.40$; $p_{\text{adjust}}=0.48$; Fig. 1C). Double mutant female NOD:*Ins1*^{Neo/Cre} mice (lacking both wildtype alleles
241 of *Ins1*) were protected from diabetes (29% diabetes incidence) when compared to NOD:*Ins1*^{WT/WT} mice
242 (64%), ($p=0.019$; $p_{\text{adjust}}=0.078$), to a similarly extent as NOD:*Ins1*^{Cre/WT} (27%) mice ($p=0.98$; $p_{\text{adjust}}=0.98$;
243 Fig. 1C). NOD:*Ins1*^{Neo/WT} mice had a significantly lower diabetes incidence than NOD:*Ins1*^{Cre/Neo} mice

244 (p=0.038; p_{adjust}=0.078; Fig. 1C) further suggesting Cre expression rather than loss of one *Ins1* allele
245 protects against diabetes onset in NOD mice. No differences were observed in random blood glucose
246 (Fig. 1D,E) and body mass (Fig. 1F,G) prior to diabetes onset in female mice. Together, these data
247 confirm previous findings that reduced *Ins1* gene dosage protects NOD mice from diabetes, but also
248 reveal a further, additive protective effect of β-cell Cre expression.

249 Male NOD:*Ins1*^{WT/WT} mice demonstrated a low diabetes incidence as expected (20% incidence), We
250 observed no cases of hyperglycemia in any of the male mice with reduced *Ins1* gene dosage (Fig. 2A).
251 There were no differences in random blood glucose (Fig. 2 B,C) or body mass (Fig. 2D,E) between any
252 of the groups. These results confirm the strong sex bias in this NOD model and suggest that the
253 protection conferred by reducing *Ins1* gene dosage may not be sex-specific.

254

255 *Insulitis and Insulin auto-antibodies*

256 Next, we examined the effects of reduced *Ins1* gene dosage and Cre expression on insulitis in female
257 mice, the pathological evidence of islet directed autoimmunity. We found no significant difference in
258 plasma insulin or autoantibodies between any of the genotypes (Fig. 3A,B). H&E-stained pancreas
259 sections (Fig. 3C) were blindly scored for immune islet infiltration in a pre-diabetic cohort of littermates
260 euthanized at 12 weeks of age, and also in the mice that survived to 1 year. Insulitis scores from 12-
261 week-old mice with reduced *Ins1* gene dosages were not significantly different from NOD:*Ins1*^{WT/WT}
262 littermates. We noticed the least amount of immune islet infiltration in double mutant NOD:*Ins1*^{Neo/Cre}
263 mice (Fig. 3D), consistent with their more complete protection from diabetes. The outcomes of the
264 samples gathered at 1 year are unfortunately inconclusive due to low sample size (NOD:*Ins1*^{WT/WT}, n=3)
265 (Fig 3E). The lower survival rate may therefore mask any potential significant changes for both insulitis
266 scoring (Fig. 3E) and insulin auto-antibodies (Fig. 3B). Unfortunately, we did not collect blood for this
267 analysis at the 12-week timepoint for all cohorts due to challenges brought about by the COVID19-
268 pandemic.

269

270 *Immune cell characterization*

271 To assess immune cell populations in the pancreatic lymph nodes and spleen at 50 weeks of age,
272 we used a panel of validated antibodies for flow cytometry. While we were able to confidently identify
273 many key immune cell populations (Fig. 4), there were no significant differences between groups (Fig.
274 5). These observations demonstrate that β -cell specific insulin gene manipulations alter type 1 diabetes
275 incidence without robust effects on the lymphocytes found in the pancreatic lymph nodes and spleen.

276

277 *Independent Validation Cohort*

278 To ensure the protective effects of β -cell Cre expression were not solely limited to a single animal
279 housing facility, we additionally studied female NOD:*Ins1*^{Cre/WT} mice that were independently generated
280 at a separate site (Fig. 6) in parallel to the cohorts studied in Figure 1. The overall incidence of diabetes
281 development in female NOD mice in this second animal colony was as expected (approximately 65-
282 80% by 25 weeks of age, Fig. 6A). Similar to our data shown in Figure 1, we observed that female
283 NOD:*Ins1*^{Cre/WT} animals were protected from diabetes incidence (25% by 1 year) and had significantly
284 improved mean blood glucose (Fig. 6C) when compared to NOD:*Ins1*^{WT/WT} littermates (75% incidence
285 by 1 year). Again, these studies confirm the protective effects of reduced *Ins1* gene dosage and β -cell
286 Cre expression in NOD mice and suggest that these findings are not due to a consequence of
287 environment or housing.

288

289 **Discussion**

290 In this study, we used a rigorous littermate control study design to examine the effects, of replacing
291 one *Ins1* allele with Cre-recombinase, on the onset of diabetes in mice of an NOD background. To
292 investigate, whether potential effects were due to the loss of *Ins1* or the introduction of Cre we included
293 *Ins1*^{Neo/WT} mice, in our study. Both *Ins1*^{Cre} and *Ins1*^{Neo} mice have reduced *Ins1* gene dosages with 50%
294 or 100% in their heterozygous and homozygous states, respectively. We found a similar reduction in
295 the diabetes incidence in female *Ins1*^{Cre/WT} mice and *Ins1*^{Neo/Cre} mice when compared to littermate control
296 *Ins1*^{WT/WT} mice. This work has implications for our understanding of the pathogenesis of type 1 diabetes,

297 as well as for the use of Cre-recombinase as a tool for *in vivo* genome engineering in mouse models of
298 the disease.

299 Our findings concur with previous work that showed a similar reduction in diabetes incidence in
300 female NOD mice lacking 1 or 2 alleles of *Ins1* (10,15), although we did not observe additional protection
301 with the double *Ins1* knockout, beyond what was seen with the Cre replacement allele. Similarly, our
302 data are in alignment with a previous study showing replacing the murine *Ins1* gene with the human *INS*
303 gene was found to protect female NOD mice from diabetes in both heterozygous and homozygous
304 states (17). We were unable to detect differences in diabetes incidence in male *Ins1*^{Cre/WT}, *Ins1*^{Neo/WT},
305 and *Ins1*^{Neo/Cre} NOD mice, perhaps due to an insufficient study period. A previous study found that
306 removal of a single *Ins1* allele is sufficient to abolish spontaneous diabetes in 50-week-old male NOD
307 mice (10). Together with the work of others, our experiments support the contention that proinsulin 1 is
308 a key player in the generation of autoimmunity in mice. While there are several autoantigens targeted
309 by autoreactive T cells in type 1 diabetes (2), insulin and proinsulin are particularly common
310 autoantibody targets in prediabetic humans (29,30). Our experiments were underpowered to detect
311 subtle differences in the levels of insulin autoantibodies, as we were limited by only examining a single,
312 late time point. However, we did examine insulitis at two time points, and insulin antibodies are often
313 correlated with insulitis (31). In our hands, there was a qualitative difference in the number of islets that
314 did not exhibit insulitis at 50 weeks in mice with at least 1 *Ins1* allele replaced. At 12 weeks, there was
315 a slight trend towards more insulitis-free islets in the *Ins1*^{Neo/Cre} mice, consistent with the greater
316 protection from type 1 diabetes incidence. These observations are consistent with previous studies
317 showing that *Ins1* knockout in NOD mice is protective against the development and severity of insulitis
318 (10). Thus, our results show that reducing the *Ins1* gene dosage lowers the threshold required for
319 diabetes onset, likely by removing the source of primary autoantigens and suppressing insulitis.

320 An important observation of our study is that Cre expression itself has protective effects in NOD mice,
321 beyond the protection afforded by the loss of 1 *Ins1* allele. To examine the specific consequences of
322 Cre expression, we compared NOD; *Ins1*^{Cre/WT} to a different knock-in (neo) *Ins1*^{Neo/WT} mouse line and
323 found roughly twice as much final diabetes protection in *Ins1*^{Cre/WT} mice versus *Ins1*^{Neo/WT} mice. Though

324 it is possible diabetes could have been delayed further than 1 year, these findings suggest that Cre itself
325 may affect diabetes rates in female NOD mice, with the caveat the Neo and Cre insertions are different,
326 altering the local gene structure. Mechanistically, we are able to attribute the observed effects to
327 differences in insulitis, suggesting the possibility of a β -cell autonomous effect of Cre expression.
328 Previous studies highlighted the potential of Cre recombinase to result in toxicity due to DNA damage
329 (32,33) Mammalian genomes contain pseudo loxP sites, and even though these sequences can deviate
330 considerably from the consensus loxP site, they can still serve as functional recognition sites for Cre
331 (32). It is predicted that the frequency of pseudo-loxP sites could be as many as 250 and 300 in mouse
332 and human genomes, respectively (33). The sustained presence of high levels of Cre in fibroblasts can
333 cause growth arrest and chromosomal abnormalities (18-20,22,23). Cre-dependent DNA damage and
334 accumulation of cytoplasmic DNA have been shown to initiate a STING-dependent immune response
335 (34). STING is an intracellular adaptor molecule, associated with the endoplasmic reticulum membrane
336 (35), that can play a critical role in detecting pathogen-derived DNA in the cytoplasm (36). There is
337 precedence for diabetes protection in NOD mice with early exposure to pathogen in the coxsackievirus
338 mode (37). A recent paper reported that STING is required for normal β -cell function in mice (38),
339 although, ironically, the study did not employ Cre-only controls. Theoretically, Cre expressed in β -cells
340 could delay the onset of diabetes in a STING-dependent manner. Future studies, beyond the scope of
341 this work, will be required to delineate the molecular mechanisms by which Cre expression induces
342 further protection that *Ins1* loss in the NOD mouse model. To unequivocally demonstrate an effect of
343 Cre activity on progression to T1D/insulitis, mice would have to be generated with enzyme-dead Cre
344 knocked into the same locus, but such studies are also beyond the scope of this work.

345 As with all studies, this work has a number of limitations. For example, the broadly observed
346 phenomenon that diabetes incidences differ between NOD mouse colonies means that we cannot
347 directly compare the results between sites. We do not know the reasons for the apparent difference in
348 diabetes incidence in wildtype NOD mice between our colonies, but it could be related to many
349 environmental factors, including native microbiome, water, food, or bedding, as well as subtle
350 differences in genotype. Another caveat of our study is that we could not simultaneously address *Ins1*

351 gene dosage and the effects of the Cre transgene, because generating both homozygous and
352 heterozygous littermates with each of the knock-in alleles is impossible. In order to reduce the potential
353 impacts of environment and genotype, mentioned above, it was imperative that we prioritized using
354 littermates. Another limitation is the natural uncertainty if *Ins1*^{Cre/WT} mice could have proceeded to
355 develop diabetes beyond the end of this study. While our study has limitations, we believe it is important
356 to report these results that will help guide those in the field who use type 1 diabetes mouse models or
357 Cre in any context.

358 In summary, our observations suggest caution when interpreting experiments that involve Cre
359 recombinase in NOD mice. Our data showed that Cre expression itself has protective effects in NOD
360 mice, beyond the protection afforded by the loss of 1 *Ins1* allele. Cre-loxP systems are vital tools for
361 research, however, there are multiple caveats that should be considered related to off-target effects and
362 the determination of correct controls. At the bare minimum, Cre-only controls are essential. Additional
363 tools for *in vivo* genome engineering are required to advance the field. Many studies will need to be re-
364 interpreted.

365

366 **Acknowledgements**

367 We thank the BC Diabetes Research community and the Johnson laboratory members for valuable
368 feedback and discussions at local meetings. We thank Dr. Liping Yu and his team at the Insulin Antibody
369 Core Lab at the University of Colorado, Barbara Davis Diabetes Centre for insulin auto-antibody
370 analysis. We thank Dr. Cara Ellis, at University of Alberta for helpful statistics discussions and analysis
371 of survival/ diabetes incidence data. We thank the amazing animal care services staff for their daily
372 attention and care of our NOD mice housed at UBC, especially during the challenging COVID-19
373 pandemic.

374

375 **Data Availability**

376 Data generated during and/or analyzed during the current study are not publicly available but are
377 available from the corresponding author on reasonable request.

378

379 **References**

- 380 1. Daniel D, Gill RG, Schloot N, Wegmann D. Epitope specificity, cytokine production profile and
381 diabetogenic activity of insulin-specific T cell clones isolated from NOD mice. *Eur J Immunol.*
382 1995;25(4):1056-1062.
- 383 2. Thebault-Baumont K, Dubois-Laforgue D, Krief P, Briand JP, Halbout P, Vallon-Geoffroy K,
384 Morin J, Laloux V, Lehuen A, Carel JC, Jami J, Muller S, Boitard C. Acceleration of type 1
385 diabetes mellitus in proinsulin 2-deficient NOD mice. *J Clin Invest.* 2003;111(6):851-857.
- 386 3. Atkinson MA, Eisenbarth GS, Michels AW. Type 1 diabetes. *Lancet.* 2014;383(9911):69-82.
- 387 4. Ehlers MR. Immune interventions to preserve beta cell function in type 1 diabetes. *J Investigig
388 Med.* 2016;64(1):7-13.
- 389 5. Makino S, Kunimoto K, Muraoka Y, Mizushima Y, Katagiri K, Tochino Y. Breeding of a non-
390 obese, diabetic strain of mice. *Jikken Dobutsu.* 1980;29(1):1-13.
- 391 6. Melanitou E, Devendra D, Liu E, Miao D, Eisenbarth GS. Early and quantal (by litter)
392 expression of insulin autoantibodies in the nonobese diabetic mice predict early diabetes
393 onset. *J Immunol.* 2004;173(11):6603-6610.
- 394 7. Gregori S, Giarratana N, Smiroldo S, Adorini L. Dynamics of pathogenic and suppressor T
395 cells in autoimmune diabetes development. *J Immunol.* 2003;171(8):4040-4047.
- 396 8. Ize-Ludlow D, Lightfoot YL, Parker M, Xue S, Wasserfall C, Haller MJ, Schatz D, Becker DJ,
397 Atkinson MA, Mathews CE. Progressive erosion of beta-cell function precedes the onset of
398 hyperglycemia in the NOD mouse model of type 1 diabetes. *Diabetes.* 2011;60(8):2086-2091.
- 399 9. Mathews CE, Xue S, Posgai A, Lightfoot YL, Li X, Lin A, Wasserfall C, Haller MJ, Schatz D,
400 Atkinson MA. Acute Versus Progressive Onset of Diabetes in NOD Mice: Potential Implications
401 for Therapeutic Interventions in Type 1 Diabetes. *Diabetes.* 2015;64(11):3885-3890.
- 402 10. Moriyama H, Abiru N, Paronen J, Sikora K, Liu E, Miao D, Devendra D, Beilke J, Gianani R,
403 Gill RG, Eisenbarth GS. Evidence for a primary islet autoantigen (preproinsulin 1) for insulitis
404 and diabetes in the nonobese diabetic mouse. *Proc Natl Acad Sci U S A.* 2003;100(18):10376-
405 10381.
- 406 11. Mehran AE, Templeman NM, Brigidi GS, Lim GE, Chu KY, Hu X, Botezelli JD, Asadi A,
407 Hoffman BG, Kieffer TJ, Bamji SX, Clee SM, Johnson JD. Hyperinsulinemia drives diet-
408 induced obesity independently of brain insulin production. *Cell Metab.* 2012;16(6):723-737.
- 409 12. Fan Y, Rudert WA, Grupillo M, He J, Sisino G, Trucco M. Thymus-specific deletion of insulin
410 induces autoimmune diabetes. *Embo J.* 2009;28(18):2812-2824.
- 411 13. Martin-Pagola A, Pileggi A, Zahr E, Vendrame F, Damaris Molano R, Snowhite I, Ricordi C,
412 Eisenbarth GS, Nakayama M, Pugliese A. Insulin2 gene (Ins2) transcription by NOD bone
413 marrow-derived cells does not influence autoimmune diabetes development in NOD-Ins2
414 knockout mice. *Scand J Immunol.* 2009;70(5):439-446.
- 415 14. Botezelli JD, Overby P, Lindo L, Wang S, Haida O, Lim GE, Templeman NM, Pauli JR,
416 Johnson JD. Adipose depot-specific upregulation of Ucp1 or mitochondrial oxidative complex
417 proteins are early consequences of genetic insulin reduction in mice. *Am J Physiol Endocrinol
418 Metab.* 2020;319(3):E529-E539.
- 419 15. Babaya N, Nakayama M, Moriyama H, Gianani R, Still T, Miao D, Yu L, Hutton JC, Eisenbarth
420 GS. A new model of insulin-deficient diabetes: male NOD mice with a single copy of Ins1 and
421 no Ins2. *Diabetologia.* 2006;49(6):1222-1228.
- 422 16. Zhang AMY, Magrill J, de Winter TJJ, Hu X, Skovso S, Schaeffer DF, Kopp JL, Johnson JD.
423 Endogenous Hyperinsulinemia Contributes to Pancreatic Cancer Development. *Cell Metab.*
424 2019;30(3):403-404.
- 425 17. Elso CM, Scott NA, Mariana L, Masterman EI, Sutherland APR, Thomas HE, Mannerling SI.
426 Replacing murine insulin 1 with human insulin protects NOD mice from diabetes. *PLoS One.*
427 2019;14(12):e0225021.

428 18. Loonstra A, Vooijs M, Beverloo HB, Allak BA, van Drunen E, Kanaar R, Berns A, Jonkers J.
429 Growth inhibition and DNA damage induced by Cre recombinase in mammalian cells. *Proc
430 Natl Acad Sci U S A.* 2001;98(16):9209-9214.

431 19. Silver DP, Livingston DM. Self-excising retroviral vectors encoding the Cre recombinase
432 overcome Cre-mediated cellular toxicity. *Mol Cell.* 2001;8(1):233-243.

433 20. Pfeifer A, Brandon EP, Kootstra N, Gage FH, Verma IM. Delivery of the Cre recombinase by a
434 self-deleting lentiviral vector: efficient gene targeting in vivo. *Proc Natl Acad Sci U S A.*
435 2001;98(20):11450-11455.

436 21. Baba Y, Nakano M, Yamada Y, Saito I, Kanegae Y. Practical range of effective dose for Cre
437 recombinase-expressing recombinant adenovirus without cell toxicity in mammalian cells.
438 *Microbiol Immunol.* 2005;49(6):559-570.

439 22. Lexow J, Poggioli T, Sarathchandra P, Santini MP, Rosenthal N. Cardiac fibrosis in mice
440 expressing an inducible myocardial-specific Cre driver. *Dis Model Mech.* 2013;6(6):1470-1476.

441 23. Bersell K, Choudhury S, Mollova M, Polizzotti BD, Ganapathy B, Walsh S, Wadugu B, Arab S,
442 Kuhn B. Moderate and high amounts of tamoxifen in alphaMHC-MerCreMer mice induce a
443 DNA damage response, leading to heart failure and death. *Dis Model Mech.* 2013;6(6):1459-
444 1469.

445 24. Li Y, Choi PS, Casey SC, Felsher DW. Activation of Cre recombinase alone can induce
446 complete tumor regression. *PLoS One.* 2014;9(9):e107589.

447 25. Sofi MH, Gudi R, Karumuthil-Meletih S, Perez N, Johnson BM, Vasu C. pH of drinking water
448 influences the composition of gut microbiome and type 1 diabetes incidence. *Diabetes.*
449 2014;63(2):632-644.

450 26. Villarreal D, Pradhan G, Wu CS, Allred CD, Guo S, Sun Y. A Simple High Efficiency Protocol
451 for Pancreatic Islet Isolation from Mice. *J Vis Exp.* 2019(150).

452 27. Bankhead P, Loughrey MB, Fernandez JA, Dombrowski Y, McArt DG, Dunne PD, McQuaid S,
453 Gray RT, Murray LJ, Coleman HG, James JA, Salto-Tellez M, Hamilton PW. QuPath: Open
454 source software for digital pathology image analysis. *Sci Rep.* 2017;7(1):16878.

455 28. Lee JTC, Shanina I, Chu YN, Horwitz MS, Johnson JD. Carbamazepine, a beta-cell protecting
456 drug, reduces type 1 diabetes incidence in NOD mice. *Sci Rep.* 2018;8(1):4588.

457 29. Kuglin B, Gries FA, Kolb H. Evidence of IgG autoantibodies against human proinsulin in
458 patients with IDDM before insulin treatment. *Diabetes.* 1988;37(1):130-132.

459 30. Yu L, Robles DT, Abiru N, Kaur P, Rewers M, Kelemen K, Eisenbarth GS. Early expression of
460 antiinsulin autoantibodies of humans and the NOD mouse: evidence for early determination of
461 subsequent diabetes. *Proc Natl Acad Sci U S A.* 2000;97(4):1701-1706.

462 31. Robles DT, Eisenbarth GS, Dailey NJ, Peterson LB, Wicker LS. Insulin autoantibodies are
463 associated with islet inflammation but not always related to diabetes progression in NOD
464 congenic mice. *Diabetes.* 2003;52(3):882-886.

465 32. Thyagarajan B, Guimaraes MJ, Groth AC, Calos MP. Mammalian genomes contain active
466 recombinase recognition sites. *Gene.* 2000;244(1-2):47-54.

467 33. Karimova M, Abi-Ghanem J, Berger N, Surendranath V, Pisabarro MT, Buchholz F. Vika/vox, a
468 novel efficient and specific Cre/loxP-like site-specific recombination system. *Nucleic Acids Res.*
469 2013;41(2):e37.

470 34. Pepin G, Ferrand J, Honing K, Jayasekara WS, Cain JE, Behlke MA, Gough DJ, BR GW,
471 Hornung V, Gantier MP. Cre-dependent DNA recombination activates a STING-dependent
472 innate immune response. *Nucleic Acids Res.* 2016;44(11):5356-5364.

473 35. Barber GN. STING: infection, inflammation and cancer. *Nat Rev Immunol.* 2015;15(12):760-
474 770.

475 36. Ishikawa H, Barber GN. STING is an endoplasmic reticulum adaptor that facilitates innate
476 immune signalling. *Nature.* 2008;455(7213):674-678.

477 37. Serreze DV, Wasserfall C, Ottendorfer EW, Stalvey M, Pierce MA, Gauntt C, O'Donnell B,
478 Flanagan JB, Campbell-Thompson M, Ellis TM, Atkinson MA. Diabetes acceleration or
479 prevention by a coxsackievirus B4 infection: critical requirements for both interleukin-4 and
480 gamma interferon. *J Virol.* 2005;79(2):1045-1052.

481 38. Qiao J, Zhang Z, Ji S, Liu T, Zhang X, Huang Y, Feng W, Wang K, Wang J, Wang S, Meng
482 ZX, Liu M. A distinct role of STING in regulating glucose homeostasis through insulin sensitivity
483 and insulin secretion. *Proc Natl Acad Sci U S A*. 2022;119(7).

484

485

486

487

488 **Figure Legends**

489 **Figure 1. *Ins1* replacement with Cre and Neo protects female NOD mice from type 1 diabetes.**

490 **(A)** Structure of the wildtype (WT) *Ins1* locus, recombinant alleles result of the neomycin (neo) targeting
491 vector, or the *Ins1* Cre locus. Created with Biorender.com. **(B)** Overview of breeding strategy. Created
492 with Biorender.com. **(C)** Kaplan-Meier plot denoting diabetes incidence in NOD mice by *Ins1* genotype,
493 including *Ins1*^{WT/WT}, *Ins1*^{Cre/WT}, *Ins1*^{Neo/WT} and *Ins1*^{Neo/Cre}. Survival analysis was performed using Log-
494 rank (Mantel-Cox) test (*p* value shown). **(D,E)** Individual and mean random blood glucose of female
495 mice. The mean blood glucose of the *Ins1*^{Neo/Cre} was significantly lower than that of the *Ins1*^{WT/WT}
496 colonies, with an adjusted *p*-value of 0.0023. Mean blood glucose of the *Ins1*^{Neo/WT} colony was higher
497 than those of the *Ins1*^{WT/WT} and *Ins1*^{Cre/WT} colonies, with adjusted *p*-values of 0.0002 and 0.0058
498 respectively. **(F,G)** Individual and mean body mass traces female mice. The mean body mass of the
499 *Ins1*^{Neo/Cre} mice was significantly lower compared to the *Ins1*^{Cre/WT} colony (adjusted *p*-value<0.0001). The
500 mean blood glucose of the *Ins1*^{Cre/WT} was also higher than the *Ins1*^{WT/WT} and the *Ins1*^{Cre/WT} colonies, both
501 with an adjusted *p*-value<0.0001. Error bars represent SEM

502

503 **Figure 2. Effects of *Ins1* replacement with Cre and Neo in male NOD mice.**

504 **(A)** Kaplan-Meier plot denoting diabetes incidence in NOD mice by *Ins1* genotype. **(B,C)** Individual and
505 mean random blood glucose in male mice. **(D,E)** Individual and mean body mass traces in male mice .
506 Error bars represent SEM.

507

508 **Figure 3. Insulitis scoring in female NOD mice with *Ins1* replacement.**

509 (A) Plasma insulin concentration Nanomolar (nM) collected at 14 weeks by cardiac puncture. (B) Mouse
510 insulin autoantibodies collected at 14 weeks by cardiac puncture, result of IAA is expressed as an index,
511 against internal standard positive and negative controls. (C) Representative images of H&E stained
512 pancreata used for insulitis scoring. Scale bars are 100 μ m. (D) Mean percent insulitis scores at 12-
513 week-old of each genotype, categorized by score, 0 - No Insulitis, 1 - Peri-Insulitis (<25%), 2 - Insulitis
514 (25-75%) and 3 - Severe Insulitis (>75%) respectively (E) 1-year-old time points. Error bars represent
515 SEM.

516

517 **Figure 4. Gating strategy for flow cytometry of pancreatic lymph node and spleen cells.**

518 (A) Singlets were obtained with use of FSC-A x FSC-H parameters and viable cells were identified by
519 selecting viability dye negative cells for subsequent analysis. The populations were subsequently split
520 into three groups of interest with dendritic cells identified by CD11c, B cells identified by CD19, and T
521 cells identified by CD3. T cells were further categorized into cytotoxic and helper phenotypes with use
522 of CD4 and CD8 markers and their respective single marker populations were assessed for activation
523 and priming status (naïve, effector, memory) with the use of CD69, CD44, and CD62L. Regulatory T
524 cell populations were further selected for with the use of a Foxp3 marker.

525

526 **Figure 5. Immune profiling in female NOD mice with *Ins1* replacement**

527 Flow cytometric analysis of cell populations within the pancreatic lymph node and spleen at 50 weeks
528 of age. (A) Percentage of CD3+ positive T cells and CD19+ B cells from the pancreatic lymph node. (B)
529 Percentage of CD11+ Dendritic cells from the pancreatic lymph node. (C) Percentage of CD8+CD4-
530 Cytotoxic T cells, CD8+CD4- T helper cells and CD4+Foxp3+ Treg cells from the pancreatic lymph
531 node. (D) Percentage of CD8+CD4+ immature cells and CD8-CD4- DN T cells from the pancreatic
532 lymph node. (E) Percentage of CD69+ Activated cytotoxic T cells from the pancreatic lymph node. (F)
533 CD44loCD62L + Naive cytotoxic T cells from the pancreatic lymph node. (G) Percentage of
534 CD44hiCD62 – Memory cytotoxic T cells from the pancreatic lymph node. (H) Percentage of
535 CD44midCD62 – Effector cytotoxic T cells from the pancreatic lymph node. (I) Percentage of CD69+

536 Activated T helper cells from the pancreatic lymph node. **(J)** CD44loCD62L + Naive T helper cells from
537 the pancreatic lymph node. **(K)** Percentage of CD44hiCD62 + Memory T helper cells from the pancreatic
538 lymph node. **(L)** Percentage of CD44midCD62 – Effector T helper cells from the pancreatic lymph node.
539 **(M)** Percentage of CD3+ positive T cells and CD19+ B cells from the Spleen. **(N)** Percentage of CD11+
540 Dendritic cells from the spleen. **(O)** Percentage of CD8+CD4- Cytotoxic T cells, CD8+CD4- T helper
541 cells and CD4+Foxp3+ Treg cells from the spleen. **(P)** Percentage of CD8+CD4+ immature cells and
542 CD8-CD4- DN T cells from the spleen. **(Q)** Percentage of CD69+ Activated cytotoxic T cells from the
543 spleen. **(R)** CD44loCD62L + Naive cytotoxic T cells from the spleen. **(S)** Percentage of CD44hiCD62 –
544 Memory cytotoxic T cells from the spleen. **(T)** Percentage of CD44midCD62 – Effector cytotoxic T cells
545 from the spleen. **(U)** Percentage of CD69+ Activated T helper cells from the spleen. **(V)** CD44loCD62L
546 + Naive T helper cells from the spleen. **(W)** Percentage of CD44hiCD62 + Memory T helper cells from
547 the spleen. **(X)** Percentage of CD44midCD62 – Effector T helper cells from the spleen. Error bars
548 represent SEM.

549

550 **Figure 6. *Ins1* replacement with Cre protects female NOD mice from type 1 diabetes in an
551 independent facility.**

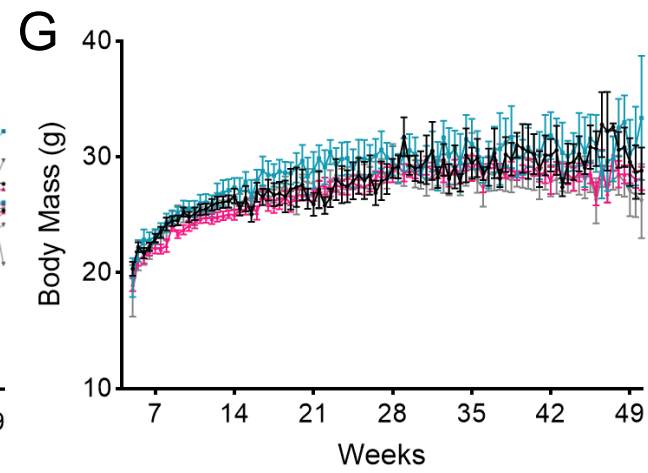
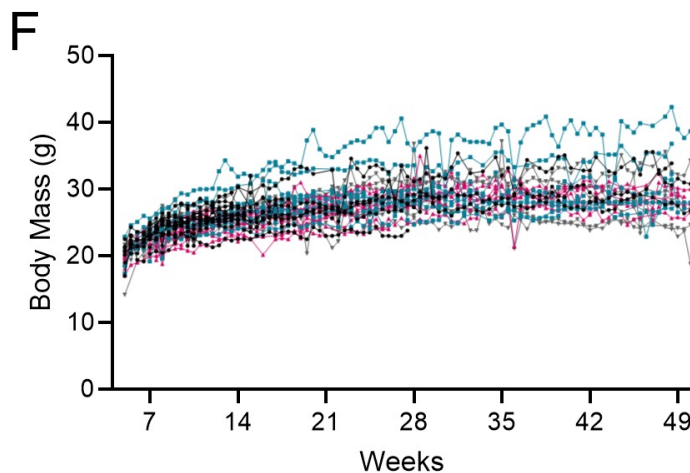
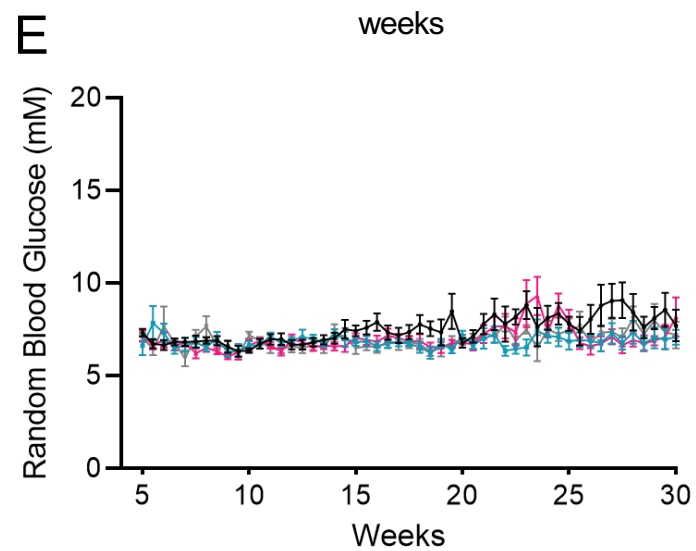
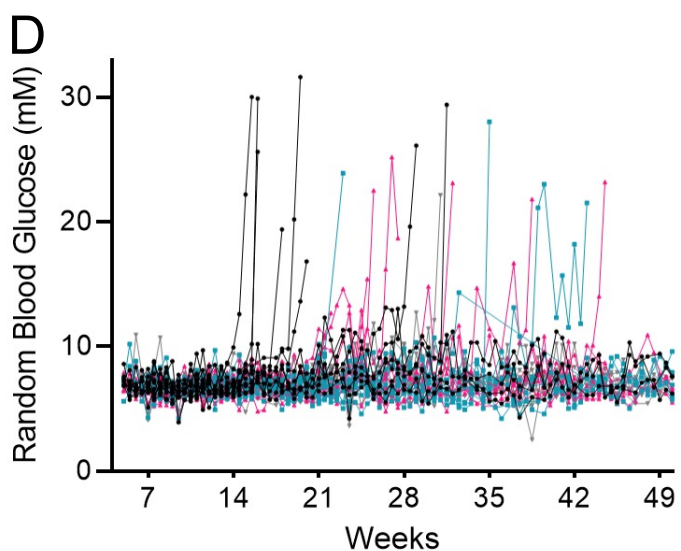
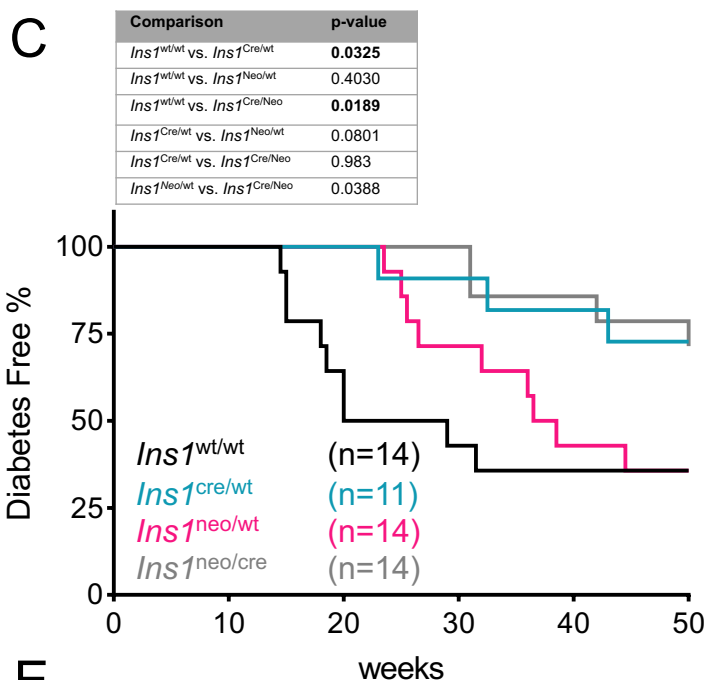
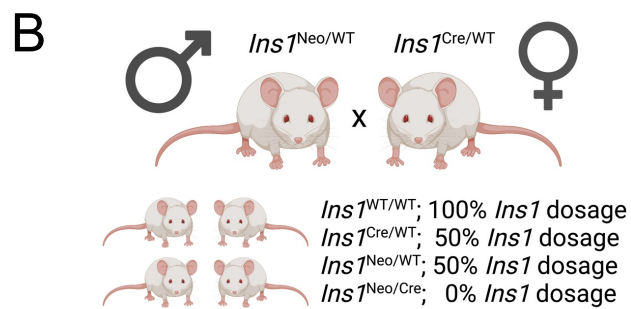
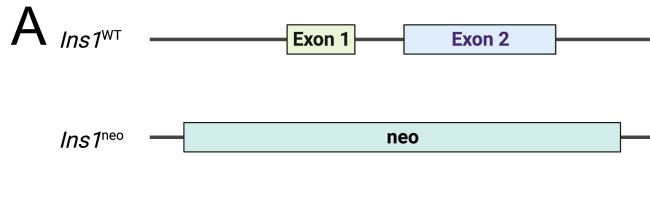
552 **(A)** Kaplan-Meier plot denoting diabetes incidence. **(B,C)** Individual and mean random blood glucose of
553 female NOD colonies from a second, independent site. The mean blood glucose of the *Ins1*^{Neo/Cre} (green)
554 was significantly lower than that of the *Ins1*^{WT/WT} (blue) littermates, with an adjusted p-value < 0.05.
555 Female NOD non-littermate controls used to track overall diabetes incidence in the colony are listed in
556 red. Error bars represent SEM.

557

558 **Table 1. Summary of Antibodies used for Flow cytometry**

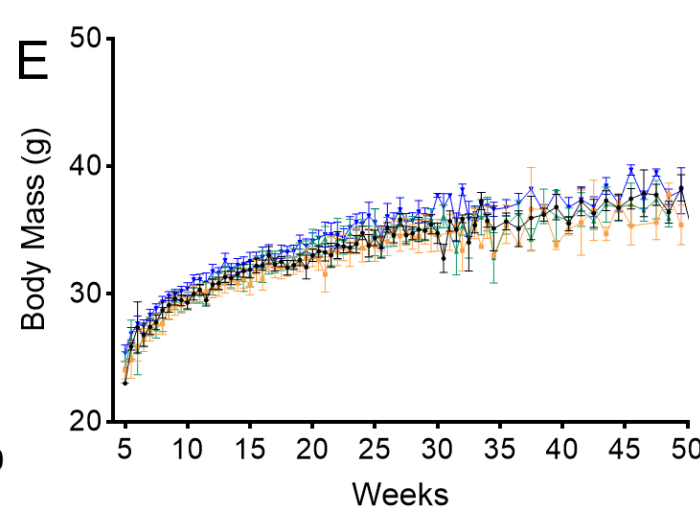
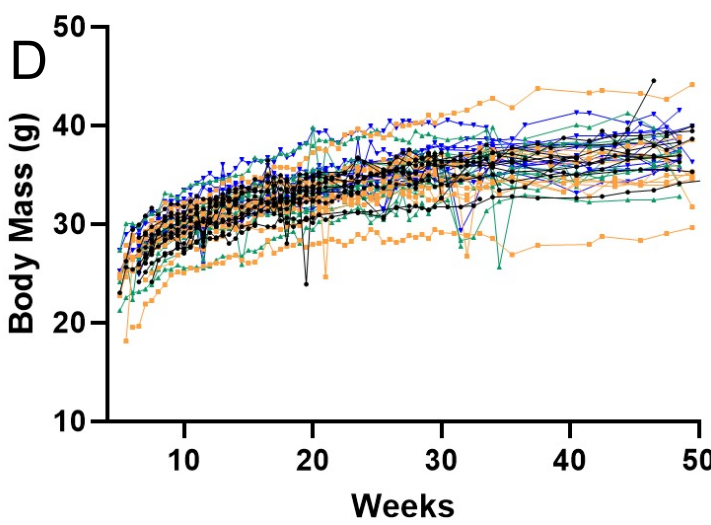
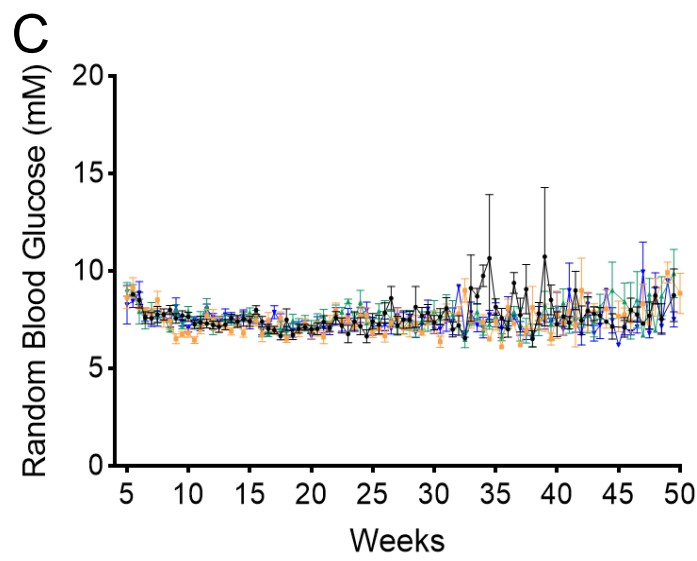
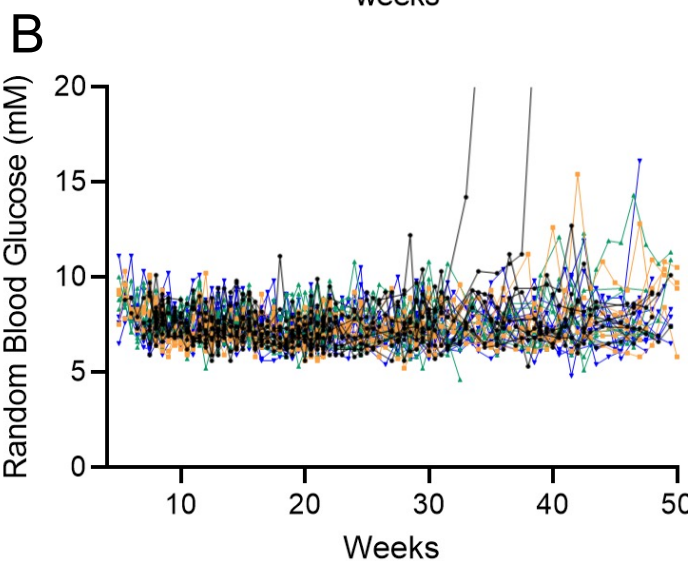
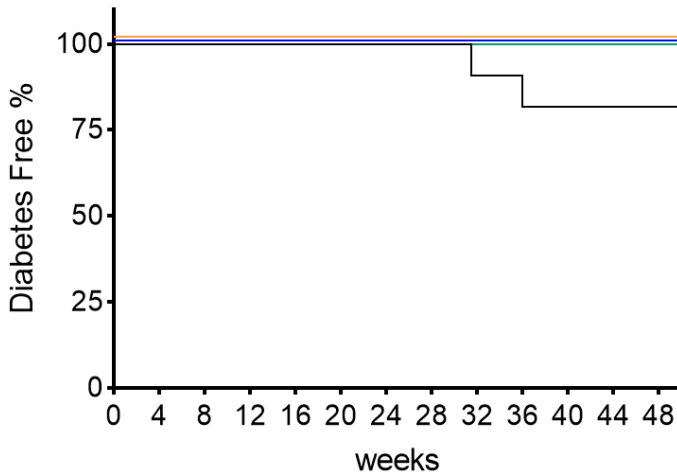
Antibody	Manufacturer	Colour	Laser (nM)	Filter	Catalogue#	RRID
CD3	ThermoFisher	e-Flour 540	405	450/45	48-003382	AB_2016704
CD4	ThermoFisher	BV650	405	660/10	64-0042-82	AB_2662401
CD8	BioLegend	PE-TR	561	610/20	100762	AB_2564027

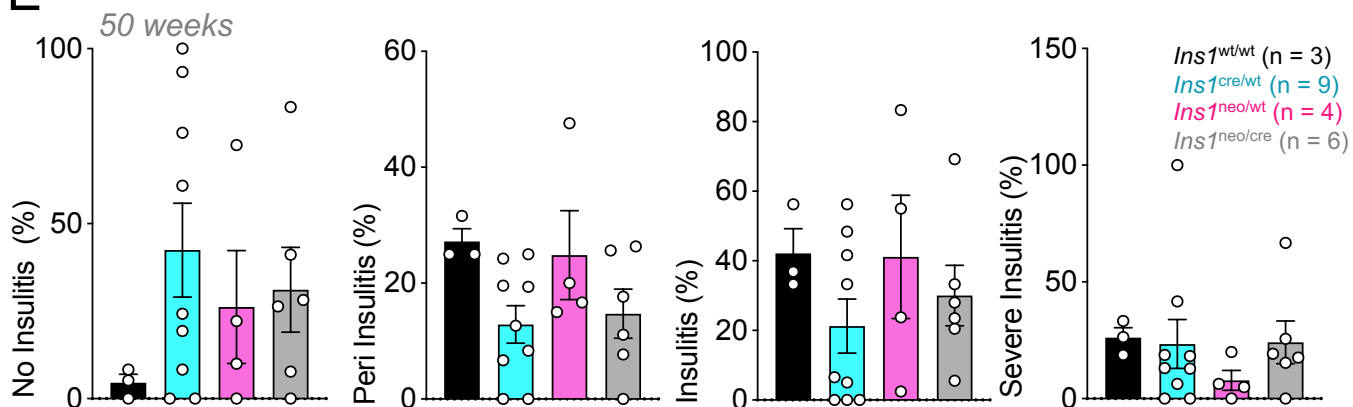
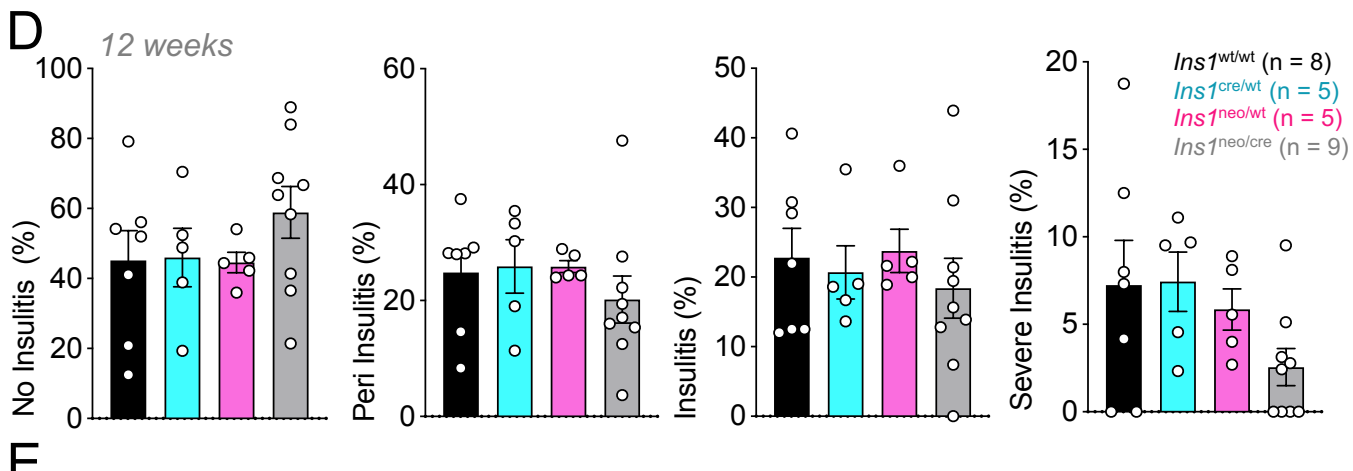
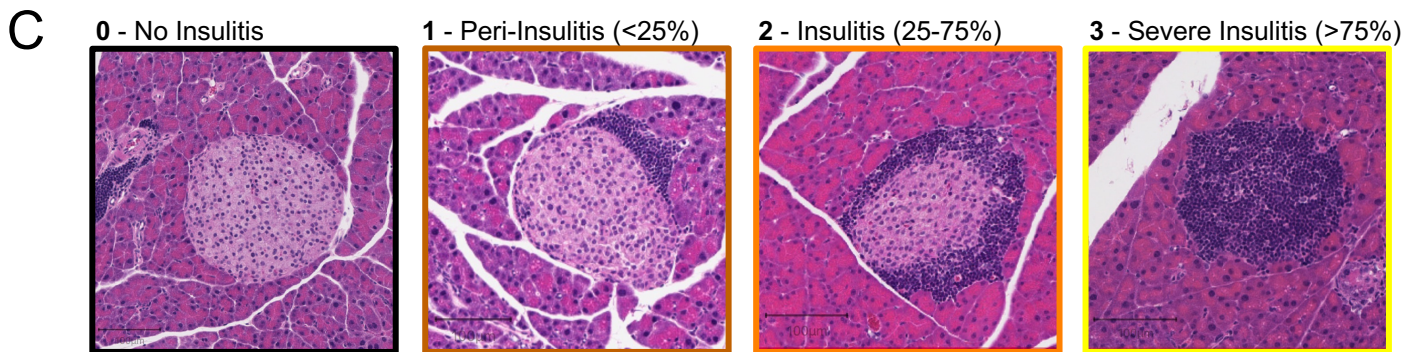
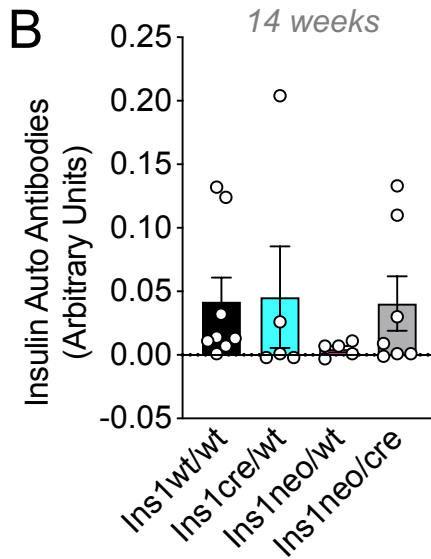
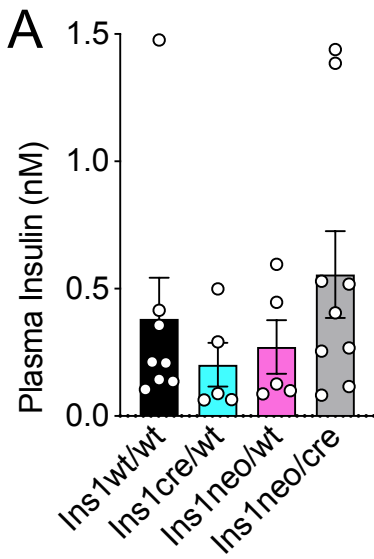
CD11c	ThermoFisher	PE	561	585/42	12-0114-81	AB_465551
CD19	ThermoFisher	SB780	405	763/43	78-0193-82	AB_2722936
CD44	ThermoFisher	APC	633	660/10	17-0441-82	AB_469390
CD62L	ThermoFisher	PerCP-Cy5.5	488	690/50	45-0621-82	AB_996667
CD69	ThermoFisher	FITC	488	525/40	11-0692-82	AB_11069282
Foxp3	ThermoFisher	AF-700	633	712/25	565773-82	AB_1210557

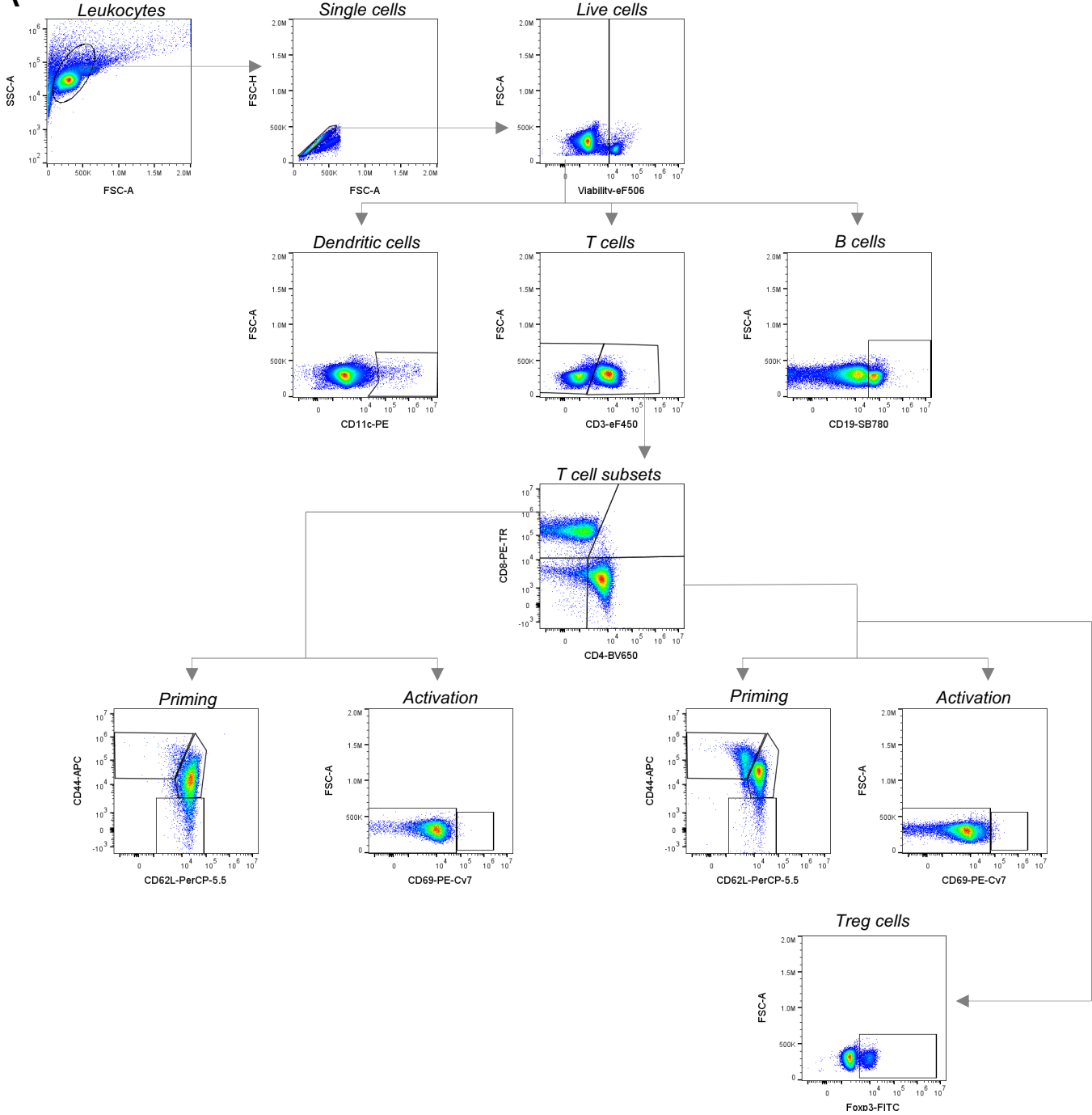


A  $Ins1^{neo/wt} \times Ins1^{cre/wt}$ 

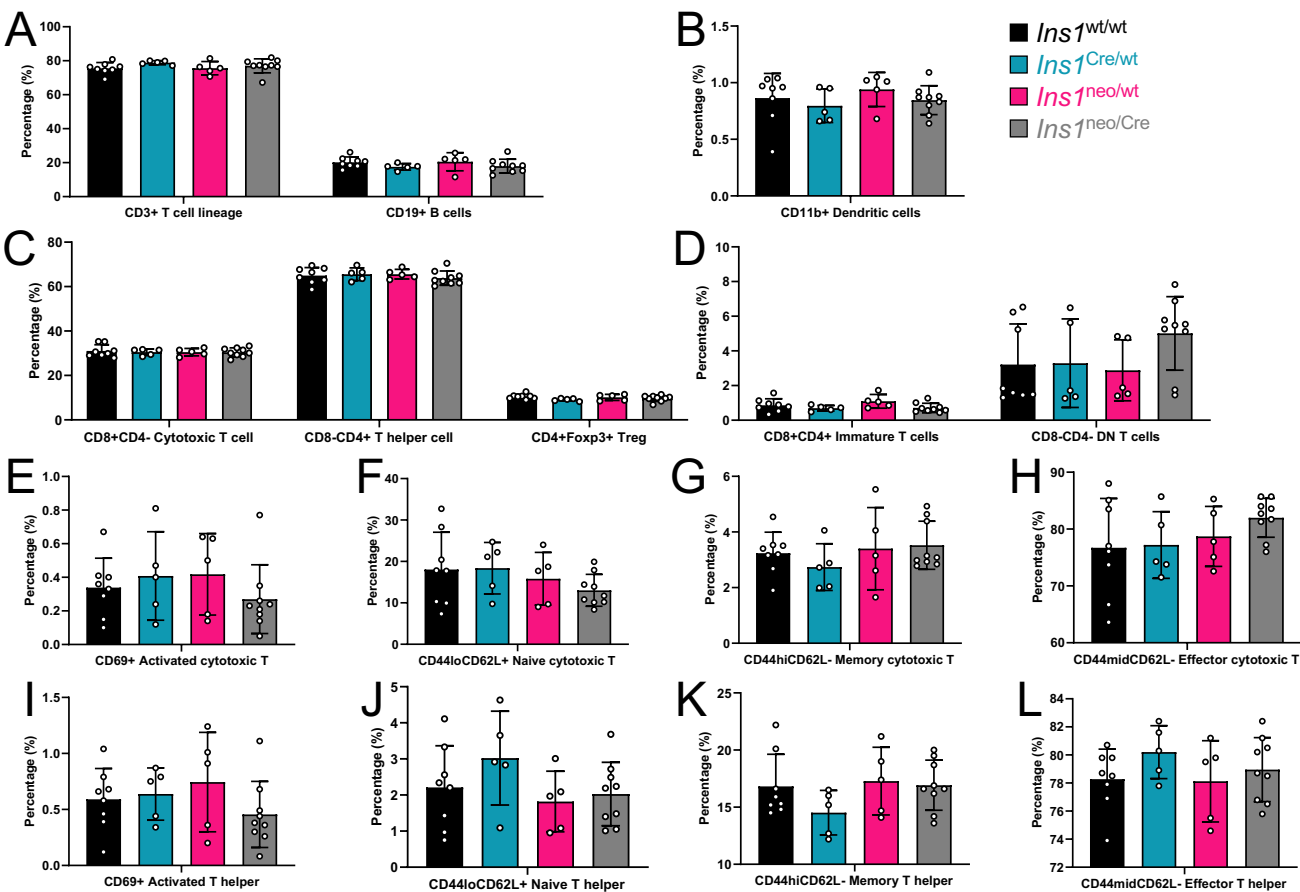
$Ins1^{wt/wt}$ (n=11)
 $Ins1^{cre/wt}$ (n=10)
 $Ins1^{neo/wt}$ (n=10)
 $Ins1^{neo/cre}$ (n=11)



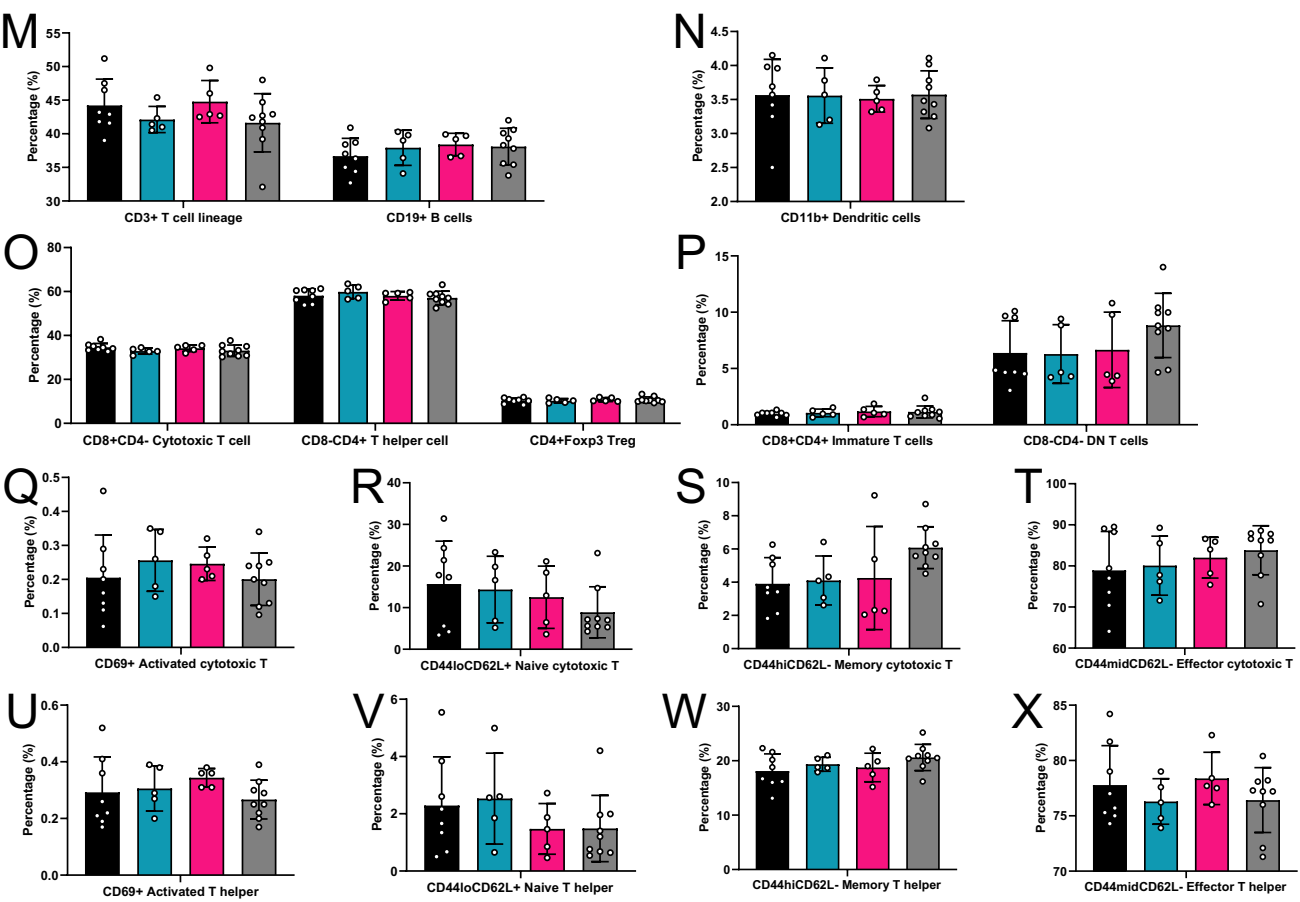


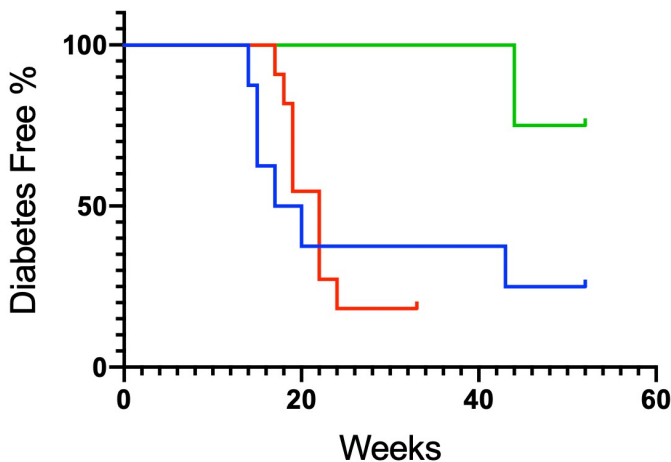
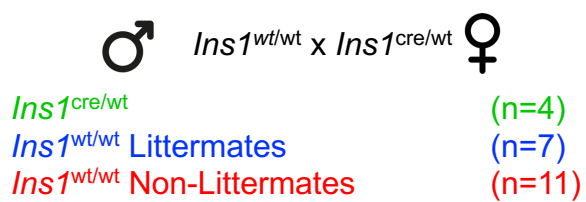
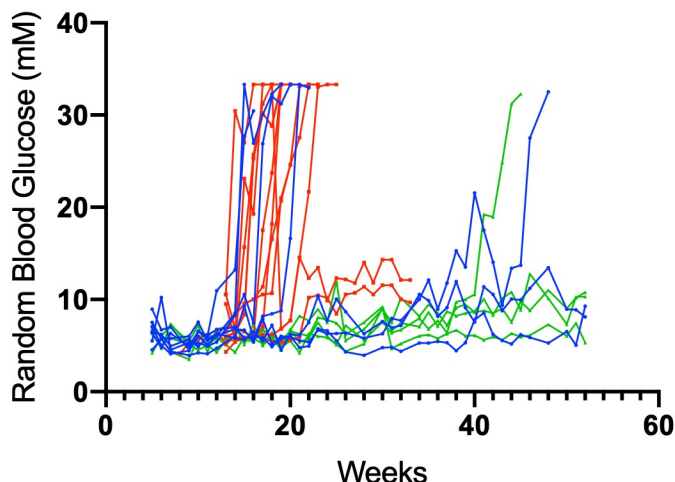
A

Pancreatic Lymph Node



Spleen



A*Michigan cohort***B****C**